Eur. Phys. J. B **16**, 59–66 (2000)

THE EUROPEAN PHYSICAL JOURNAL B

EDP Sciences

Structural instability and superconductivity in $Ba_{1-x}K_xBiO_3$

S. Zherlitsyn[1,2], B. Lüthi[1,a], V. Gusakov[3], B. Wolf[1], F. Ritter[1], D. Wichert[1], S. Barilo[3], S. Shiryaev[3], C. Escribe-Filippini[4], and J.L. Tholence[4]

[1] Physikalisches Institut, Universität Frankfurt, 60054 Frankfurt, Germany
[2] Institute for Low Temperature Physics and Engineering, 310164 Kharkov, Ukraine
[3] Institute of physics of Solids and Semiconductors, 220072 Minsk, Belarus
[4] Laboratoire d'Études des Propriétés Électroniques des Solides, CNRS, 38042 Grenoble, France

Received 25 June 1999 and Received in final form 14 February 2000

Abstract. We report results of the ultrasonic investigation of $Ba_{1-x}K_xBiO_3$ superconducting (SC) single crystals for two potassium concentrations $x \cong 0.35$ and $x \cong 0.47$ in a wide temperature range including the normal and the SC states. An instability of the crystal lattice that develops above the superconducting phase transition leads to a softening of both the transverse c_{44} and the longitudinal c_{11} modes at temperatures between 200 K and 50 K. In the case of $Ba_{0.65}K_{0.35}BiO_3$ a pronounced hysteresis was discovered. Low temperature X-ray powder diffraction analysis does not reveal any change of the cubic structure in the samples within a resolution of our X-ray technique. The softening of the elastic moduli, the hysteresis, the maximum in the attenuation of sound along with the possible short- (or long-) range structural distortion can be explained qualitatively in a simple model by assuming a coupling of the acoustic modes with the anharmonic oscillations of BiO_6 octahedra. Some weak anomalies are discovered in the velocity of the longitudinal sound in the vicinity of the superconducting phase transition.

PACS. 62.65.+k Acoustical properties of solids – 74.72.-h High-T_c compounds

1 Introduction

The copper-free $Ba_{1-x}K_xBiO_3$ high temperature superconductor has the highest temperature of superconducting phase transition ($T_c \cong 32$ K, $x \cong 0.37$) for non copper oxides. This superconductor is a suitable object for studying the high temperature superconductivity phenomena since it places between the high temperature copper oxides superconductors and the conventional superconductors. It has a cubic symmetry for the potassium concentration $x \gtrsim 0.35$ [1]. In addition, $Ba_{1-x}K_xBiO_3$ is diamagnetic and does not exhibit any static magnetic order. A number of investigations, including oxygen isotope effect experiments [2], inelastic neutron scattering [3,4], and tunneling spectroscopy [5–7] have shown the significant role which phonons play in the superconducting mechanism of these compounds. The pairing mediated by electronic excitations [8] and the bipolaronic model [9] have been discussed too.

It is generally conceded that the unique properties of these compounds are mainly determined by the BiO_6 octahedra. The conducting band of $Ba_{1-x}K_xBiO_3$ consists mainly of antibonding combinations of Bi($6s$) and O($2p$) electronic states [10]. Oxygen oscillations associated with some optical phonons modulate the Bi-O bond length. An important role of the different phonon modes of BiO_6 octahedra in the electron-phonon interaction has been already emphasized [11–13]. In $Ba_{1-x}K_xBiO_3$ potassium ions are randomly distributed over the Ba sites [1]. The different potassium concentrations stabilize different distortions of the BiO_6 octahedra that results in a number of the crystallographic structures [1]. So far the superconductivity has been observed in $Ba_{1-x}K_xBiO_3$ in the cubic phase (space symmetry group Pm $\overline{3}$m) which persists at any temperatures for the potassium concentrations $0.35 \leq x \leq 0.5$, although an existence of a weak long range superstructure characterized by BiO_6 octahedra rotations has been also reported [14] for some SC samples. The highest critical temperature of the superconducting phase transition T_c is discovered in the vicinity of the phase boundary between the cubic and orthorhombic phases in the $x - T$ phase diagram [1]. The cubic to orthorhombic phase transition is associated in these materials with frozen BiO_6 tilting and in this case the optical R_{25} phonon mode at the [111] corner of the cubic Brillouin zone is soft [15]. Structural fluctuation with a symmetry of this mode was observed in the diffuse electron scattering in the cubic phase of $Ba_{1-x}K_xBiO_3$ [15]. The fluctuation is enhanced remarkably in the cubic phase with approaching the superconducting phase transition. Other experimental methods like the pair distribution function analysis in the neutron-diffraction experiments [16], NMR [17], and the EXAFS

[a] e-mail: luethi@physik.uni-frankfurt.de

investigations [11,18] show the presence of local distortion of the cubic structure in $Ba_{1-x}K_xBiO_3$. This distortion implies short-range ionic displacements possibly without a long range correlation between them. As a result the local symmetry is lower whereas the integral methods of structural analysis, like X-ray or neutron diffraction, could not reveal a change of the structure. An analysis of EXAFS data led the authors of reference [18] to the conclusion that a local disorder has a form of a rotation of the oxygen octahedra around the pseudocubic axes of the type [110] or [111]. A reason for the local distortion lies in strong anharmonicity of some BiO_6 octahedra oscillations.

The ultrasonic investigation is a powerful method for studying different lattice instabilities. Previous ultrasonic study [19] performed on polycrystalline samples of $Ba_{1-x}K_xBiO_3$ showed a broad minimum in the temperature dependence of the sound velocity both for the transverse and the longitudinal modes at temperature of about 40 K. In order to clarify the role of the lattice and different structural instabilities in physical properties of these compounds we carry out the ultrasonic and low temperature X-ray powder diffraction investigation of $Ba_{0.65}K_{0.35}BiO_3$ material for two potassium concentrations $x \cong 0.35$ and $x \cong 0.47$. At low temperatures the compound with $x \cong 0.35$ is situated near the line separating cubic and orthorhombic phases in the $x - T$ phase diagram, whereas $Ba_{0.53}K_{0.47}BiO_3$ is far away from the orthorhombic phase at any temperature.

2 Experimental results

In our investigation we used single crystals grown in different laboratories (Institute of Solid State Physics, Minsk ($x \cong 0.35$) and LEPES, Grenoble ($x \cong 0.47$)). Similar electro-deposition growth method was used in both cases [20,21].

The crystals had a size of about $1.5 \times 1.2 \times 1\ mm^3$. For the magnetic ac-susceptibility measurements (not shown here) we found that both of the crystals were superconductors with the onset of the superconducting phase transition at $T_c \cong 31.7$ K and the transition width $\cong 6$ K in $Ba_{0.65}K_{0.35}BiO_3$ and the onset at $T_c \cong 24$ K and the width $\cong 2$ K in $Ba_{0.53}K_{0.47}BiO_3$. We utilized resonance $LiNbO_3$ transducer with the fundamental frequency of 10 MHz glued by the liquid polymer (Thiokol-32) in the case of the transverse sound. A wide frequency band piezoelectric film glued on the samples with a two component epoxy was used for the excitation of the longitudinal sound waves. The experimental ultrasonic technique was described elsewhere [22].

The single crystals utilized in the ultrasonic investigation were cut and used in X-ray powder diffraction experiments in the temperature range between 20 K and 300 K. These diffraction experiments were carried out using a Siemens D500 powder diffractometer with Cu $K_{\alpha 1}$ radiation ($\lambda = 1.540598$ Å) equipped with a closed cycle helium refrigerator. The lattice parameters were determined to be $a = 4.295$ Å for $x \cong 0.35$ and $a = 4.270$ Å for $x \cong 0.47$ at 300 K. Low temperature diffraction experiments revealed an absence of the structural phase transition down to 20 K for both compounds within a resolution of our X-ray technique. Figure 1 exhibits X-ray powder diffraction data obtained at 300 K (upper panel) and 20 K (lower panel) in $Ba_{0.65}K_{0.35}BiO_3$. Neither extra peaks nor any visible change in linewidth were observed at low temperatures (see inset of Fig. 1). It means that if a long range distortion of cubic structure exists it should be very small at least below the resolution of our X-ray technique.

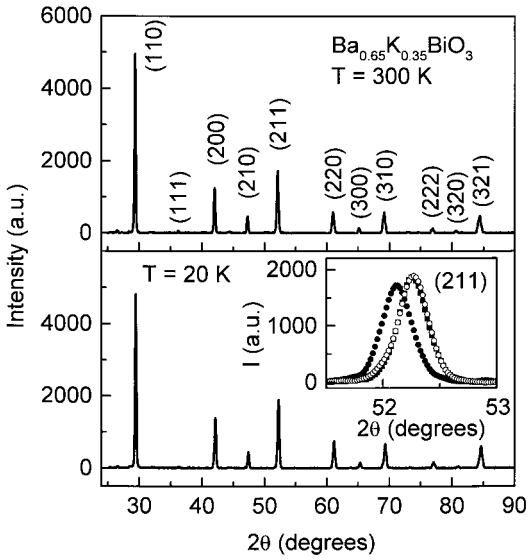

Fig. 1. X-ray powder diffraction data plots at 300 K (upper panel) and 20 K (lower panel) for $Ba_{0.65}K_{0.35}BiO_3$. Diffraction indices are also shown. Cooper $K_{\alpha 1}$ line with wave length $\lambda = 1.540598$ Å was used. Inset shows intensity of (211) reflection measured at 300 K (solid circles), 120 K (solid squares), and 20 K (open circles).

Figure 2 shows the temperature dependence of the sound velocity of the longitudinal c_{11} mode ($\mathbf{k}//\mathbf{u}//[100]$, $\mathbf{k}$ is the wave vector and $\mathbf{u}$ the polarization of the sound wave) in $Ba_{0.65}K_{0.35}BiO_3$, measured both with cooling the sample down and heating it up. There is a large softening (about 7% in the sound velocity) below 150 K with a minimum at 70 K. The anomaly in the sound velocity is accompanied by a maximum in the attenuation of sound (see Fig. 3). A hysteresis occurs in the temperature range between 50 K and 250 K for both the sound velocity and the attenuation of sound. The sound velocity behavior is steplike at 100 K for temperature sweep up, whereas the curve is smoother for temperature sweep down. The maximum in the attenuation is more prominent for the curve which corresponds to increasing temperature. A hysteresis loop is also shown in Figures 2 and 3 for the thermal cycle when the sample was heated only up to 180 K and then cooled down again. In the case of this thermal cycle the hysteresis loop becomes much narrower. We have also measured a temperature behavior of the transverse c_{44} mode ($\mathbf{k}//[100]$, $\mathbf{u}//[001]$) in $Ba_{0.65}K_{0.35}BiO_3$ (see Fig. 4). Temperature dependence of the sound velocity of this mode is slightly different from the behavior of the longitudinal

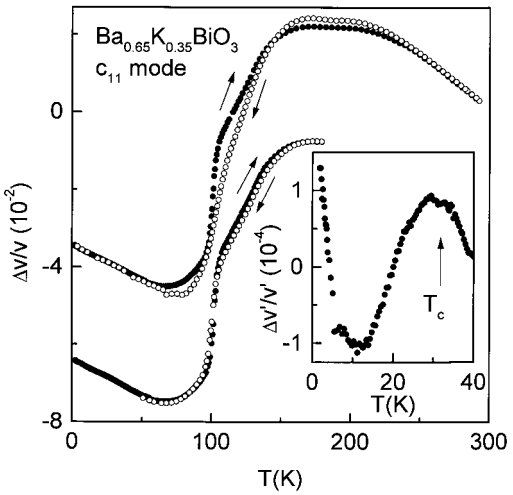

Fig. 2. Temperature dependence of the sound velocity of the longitudinal c_{11} mode in $Ba_{0.65}K_{0.35}BiO_3$. Temperature sweep up (solid symbols) and sweep down (open symbols) are shown. Two lower curves demonstrate a change in the width of the hysteresis loop in case when the sample was heated only up to 180 K and then cooled again down. The data for the two different thermal cycles (final temperatures 180 K and 292 K) were shifted arbitrarily along the ordinate axis for the sake of clarity. The ultrasound frequency was 48 MHz. Inset shows behavior of the sound velocity of the c_{11} mode in the vicinity and below of the superconducting phase transition ($T_c \cong 32$ K) after subtraction of the linear background from the data. The arrow shows the onset of the SC phase transition determined from the ac magnetic susceptibility measurements.

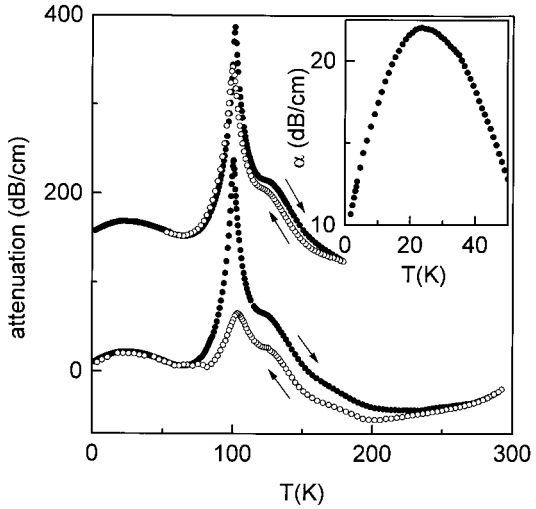

Fig. 3. Temperature dependence of the attenuation of sound of the c_{11} mode in $Ba_{0.65}K_{0.35}BiO_3$. This data was measured simultaneously with the sound velocity dependencies shown in Figure 2 at the same frequency. The two upper curves correspond to the thermocycling procedure described in Figure 2 caption for the two lower curves. The data for the two different thermal cycles were shifted arbitrarily. The meaning of solid and open symbols is the same as in Figure 2. Inset shows a low temperature behavior of the sound attenuation of the c_{11} mode.

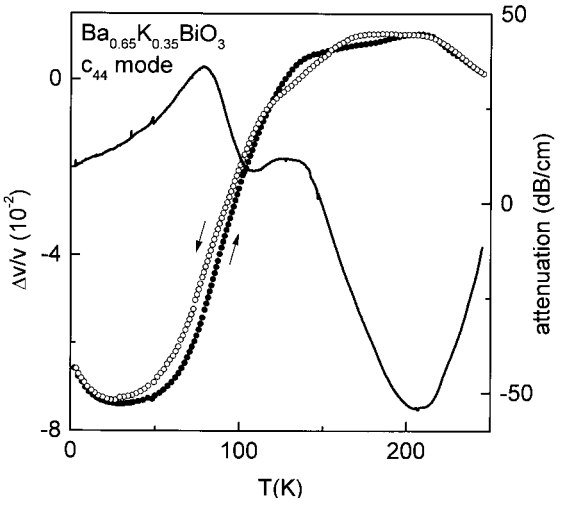

Fig. 4. Temperature dependence of the sound velocity (symbols) and the attenuation of sound (solid line) of the transverse c_{44} mode ($\mathbf{k}$//[100], $\mathbf{u}$//[001]) in $Ba_{0.65}K_{0.35}BiO_3$. For the sound velocity temperature sweeps up and down, and for the attenuation only a sweep up is shown. The ultrasonic frequency is 10 MHz.

c_{11} mode. Although there is approximately the same total (∼8% in the sound velocity) softening and the temperature hysteresis exists, there is not any more the step-like behavior at 100 K neither for the temperature sweep up nor for the temperature sweep down. Below 120 K an opposite path tracing the hysteresis loop takes place for the c_{44} mode in comparison with the c_{11} mode.

In contrast to $Ba_{0.65}K_{0.35}BiO_3$, the sound velocity of the c_{11} mode in $Ba_{0.53}K_{0.47}BiO_3$ demonstrates a rather smooth temperature behavior (see Fig. 5a). The softening begins at 250 K and ends in a minimum at 33 K. The total change in the sound velocity is approximately the same (∼7%) as for $Ba_{0.65}K_{0.35}BiO_3$. The attenuation of the c_{11} mode passes through the broad maximum at 135 K (see Fig. 5b). The hysteresis has almost completely disappeared in $Ba_{0.53}K_{0.47}BiO_3$.

Thus $Ba_{0.65}K_{0.35}BiO_3$ and $Ba_{0.53}K_{0.47}BiO_3$ show some difference in the behavior of the longitudinal acoustic mode. There is an abrupt change of the elastic constant accompanied by hysteresis in the former case, and a smooth softening in the latter case. All these anomalies can testify to the presence of the structural instability in the system for both potassium concentrations. The instability is larger if the system is closer to the cubic to orthorhombic structural phase transition (the case of $Ba_{0.65}K_{0.35}BiO_3$ compound).

There is no sharp anomaly in the sound velocity at the superconducting critical temperature T_c. One can see a significant linear term in the longitudinal sound velocity in $Ba_{0.65}K_{0.35}BiO_3$ below 60 K (see Fig. 2). In order to extract some details of the sound velocity behavior in the vicinity of T_c in this compound we found a temperature dependent background as a linear fit of the experimental data at temperatures below 56 K and then

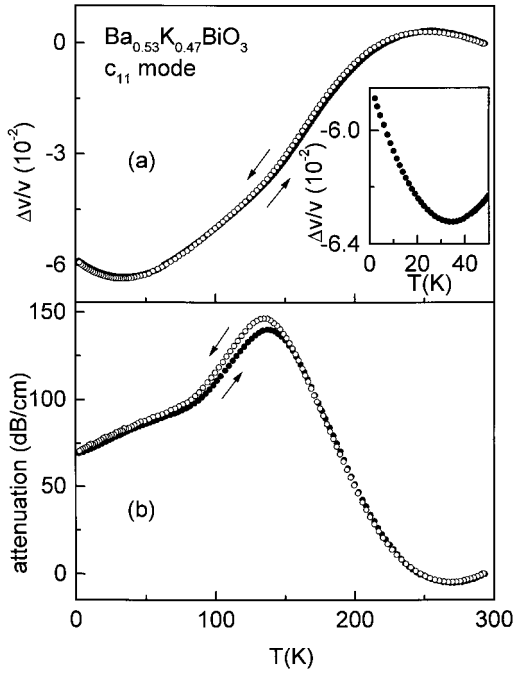

Fig. 5. Temperature dependence of the sound velocity (a) and the attenuation of sound (b) of the longitudinal c_{11} mode in $Ba_{1-x}K_xBiO_3$. Open circles correspond to decreasing and solid circles to increasing temperature. Inset shows a behavior of the sound velocity of the c_{11} mode in the vicinity of the superconducting phase transition ($T_c \cong 24$ K). The ultrasound frequency is 53 MHz.

subtracted this line from the experimental data. The result is shown in the inset of Figure 2. Note that the scale on the vertical axis in the inset is about 10^{-2} times that in Figure 2. The temperature dependence of the sound velocity demonstrates a fine structure if the linear temperature background is subtracted. In particular, there is a kink in the vicinity of T_c and then a small relative decrease in the sound velocity. The curve passes through a minimum at 12 K and retrieves its value at lowest temperatures. According to the thermodynamic consideration of the second order SC phase transition a discontinuous softening may occur for longitudinal acoustic modes [23]. The magnitude of the sound velocity change is determined by the magnitude of the linear strain dependence of T_c. In addition, below T_c the sound velocity has to have an other slope than in the normal state. Shear waves do not show any discontinuity in magnitude of the sound velocity and the discontinuity in temperature slope is determined by the quadratic strain dependence of T_c. There is no visible discontinuity in magnitude of the longitudinal sound velocity at the transition. It is not clear if the observed change in a slope of the sound velocity in the vicinity of T_c is associated with the forming of the SC state. We would like to point out that the rather broad SC phase transition in our case can mask an effect in elastic properties. We do not have any information on a strain or pressure dependence of the critical temperature and we cannot estimate a value of the sound velocity change predicted by theory. We can conclude from our experimental data that such a discontinuity should be less than 5×10^{-5}. Below 25 K the sound velocity changes approximately linearly with temperature down to 14 K. Then an unknown mechanism leads to an additional stiffening of the c_{11} elastic modulus at lowest temperatures. An alternative thermodynamics, assuming Ehrenfest fourth order SC phase transition in $Ba_{1-x}K_xBiO_3$ has been suggested recently [24] (but see also Ref. [25]).

The attenuation of sound of the c_{11} mode exhibits a shallow broad maximum at temperatures just below T_c (see insert of Fig. 3). Then the attenuation decreases without any sign of saturation down to the lowest measured temperature of 2 K. Such behavior is not typical for the SC phase transition and SC state (see, for example, Ref. [26]). But again we cannot assert that this behavior is related to superconductivity or caused by other reasons. Neither the sound attenuation of the c_{44} mode in $Ba_{0.65}K_{0.35}BiO_3$ nor the attenuation of the c_{11} mode in $Ba_{0.53}K_{0.47}BiO_3$ show any peculiarity in the vicinity of T_c (see Fig. 4, Fig. 5b). It is interesting to compare our results with the results of the ultrasonic investigation of the related compound $BaPb_{1-x}Bi_xO_3$ [27]. This compound has a set of similar structures as a function of Bi concentration x, and becomes a superconductor below 12 K. In reference [27] only the superconducting state was studied and temperature dependence of the sound velocity and the attenuation of sound looks quite different from the one shown in inserts of Figures 2 and 3.

3 Discussion

Now we shall discuss some possible physical reasons for the softening of the c_{11} and c_{44} modes in $Ba_{1-x}K_xBiO_3$ (see Figs. 2, 4, 5a). In spite of the fact that our low temperature X-ray powder diffraction experiments failed to detect any change of cubic structure we cannot completely rule out some slight orthorhombic or tetragonal distortion of the cubic lattice (first of all in the case of $Ba_{0.65}K_{0.35}BiO_3$) which is beyond the resolution of our X-ray technique. Both our samples exhibit superconductivity observed in the cubic phase, although, as we have mentioned above, some long range superstructure in superconducting samples was also reported [14]. If the structural phase transformation happens a renormalization of the sound velocity and the attenuation of sound may stem from the coupling of the order parameter to the deformation. In this case an analysis is similar to one performed long ago for the phase transition with a soft R_{25} optical phonon mode [28]. The coupling terms in the thermodynamic potential linear in strain and quadratic in the optical mode displacement [15,28] should lead to step-like anomalies in the corresponding elastic constants and velocities of sound at the critical temperature. But even so there is the question about the huge temperature range (50 − 250 K) where acoustic anomalies were observed and unusual hysteretic behavior in this temperature range. The temperature dependence of the c_{11} mode for $x = 0.35$ could indicate a structural transition at $T = 100$ K, but this is not the case

for the c_{44} mode indicating another reason for anomalous behavior. Analysing temperature dependences of the elastic constants in the paradistortive phase above the structural phase transition in some hexahalometallates Henkel *et al.* [29] considered a model based on the elastic strain coupling to the fluctuations of the soft mode coordinates. Assuming very large fluctuation area in $Ba_{1-x}K_xBiO_3$ we tried to fit our experimental data in frame of this model. We could not get any reasonable agreement to the experimental data for our compounds. Also a deformation potential analysis [30] does not give satisfactory results.

Here we shall discuss a mechanism which can result in the observed ultrasonic anomalies. This mechanism is related to the large anharmonicity of some optical oscillations [11,13,17,18] that could also be a reason for the structural transition in $Ba_{1-x}K_xBiO_3$ compounds. We present a simple model which explains the salient features of our experimental results. The peculiarities in the sound velocity and the attenuation of sound can be linked to the particular dynamics of oxygen octahedra. In $Ba_{1-x}K_xBiO_3$ oxygen atoms move in an anharmonic double-well potential originating, for instance, from an existence of two nonequivalent bismuth positions Bi(I) and Bi(II) [11] or from the results of potassium substitution on the barium sites. The two bismuth positions are associated with the presence of a pair of holes in a hybridized antibonding Bi(I)($6s$)–O($2p_\sigma$) orbital and an absence of such holes in Bi(II)($6s$)–O($2p_\sigma$) orbital. A dynamic interchange $BiO_6 \leftrightarrow BiO_6$ between the positions is also possible. Movement of oxygen atoms in double-well potential results in a rearrangement of the oxygen octahedra with variation of temperature. That leads to the renormalization of the elastic constants and to the observed anomalies in the sound velocity and the attenuation of sound. Correlation between the local ordering can lead the system to the structural transformation.

To consider this effect more rigorously let us introduce the configuration coordinate q which describes a local dynamics of oxygen octahedra in double well potential. It was shown [31,32] that for crystal lattice with a sublattice (or group of atoms) moving in a double-well potential the renormalized frequencies of crystal lattice can be presented in the following form:

$$\tilde{\omega}_k(T) = \omega_k(T) + \omega_k(T)\left[\lambda_3\left(\sigma + \langle q\rangle^2\right) - \lambda_4\frac{\left(\sigma + 4\langle q\rangle^2\right)}{m\Omega^2}\right], \tag{1}$$

where $\tilde{\omega}_k$ is a frequency of acoustic waves in the crystal with the selected sublattice moving in the anharmonic potential. $\omega_k(T)$ is a temperature dependent ultrasonic frequency without renormalization by anharmonicity. $\langle q\rangle$ is an average displacement of an atom in the anharmonic potential (in case of the harmonic approximation $\langle q\rangle = 0$), $\sigma = \langle q^2\rangle - \langle q\rangle^2$, Ω is an effective frequency of oscillations in the anharmonic potential, λ_3 and λ_4 are coupling constants which characterize cubic and quartic interactions of the main lattice with the anharmonic sublattice. A temperature dependence of the sound velocity ($v \propto \tilde{\omega}$) is determined by the renormalization function in square brackets of equation (1).

Our main task now is to calculate the temperature dependence of $\langle q\rangle(T)$, $\sigma(T)$, and $\Omega(T)$. For this purpose we use the variation inequality [33]:

$$F \le F_0 + \langle H - H_0\rangle_0, \tag{2}$$

here H is the full Hamiltonian of the system; H_0 is the approximated Hamiltonian (see below); F is the free energy of the system, described by the Hamiltonian H; F_0 is the free energy of the system with the Hamiltonian H_0; $\langle\ \rangle_0$ means averaging over H_0. We represent here oscillations in the anharmonic potential at fixed temperature as oscillations in the effective shifted harmonic potential. In this approach H and H_0 can be written as:

$$H = \frac{p^2}{2m} + \frac{\alpha}{2}q^2 - \frac{\beta}{3}q^3 + \frac{\gamma}{4}q^4,$$
$$H_0 = \frac{p^2}{2m} + \frac{m\Omega(q - \langle q\rangle)^2}{2}. \tag{3}$$

Then inequality (2) can be represented as:

$$F \le k_\mathrm{B}T\ln\left(2\mathrm{sh}\left(\frac{\hbar\Omega}{2k_\mathrm{B}T}\right)\right) + \left(\frac{\alpha}{2}\langle q\rangle^2 - \frac{\beta}{3}\langle q\rangle^3 + \frac{\gamma}{4}\langle q\rangle^4\right) + \left(\frac{\alpha}{2} - \beta\langle q\rangle + \frac{3}{2}\langle q\rangle^2\gamma - \frac{m\Omega^2}{2}\right)\sigma + \frac{3}{4}\gamma\sigma^2 \tag{4}$$

where $\sigma = \langle(q - \langle q\rangle)^2\rangle_0 = \frac{\hbar}{2m\Omega}\mathrm{cth}\left(\frac{\hbar\Omega}{2k_\mathrm{B}T}\right)$.
Minimization of the right side of the inequality (4) gives the following system of equations for the temperature dependence of the average displacement $\langle q\rangle(T)$ and the effective frequency $\Omega(T)$:

$$-(3\langle q\rangle\gamma - \beta)\frac{\hbar}{2m\Omega}\mathrm{cth}\left(\frac{\hbar\Omega}{2k_\mathrm{B}T}\right) = \alpha\langle q\rangle - \beta\langle q\rangle^2 + \gamma\langle q\rangle^3$$
$$m\Omega = \alpha - 2\beta\langle q\rangle + 3\gamma\left[\langle q\rangle^2 + \frac{\hbar}{2m\Omega}\mathrm{cth}\left(\frac{\hbar\Omega}{2k_\mathrm{B}T}\right)\right]. \tag{5}$$

Temperature dependence of the attenuation of ultrasound can be calculated in the actual case when $\omega_\mathrm{s}\tau_\mathrm{th} \ll 1$ using the following expression [34]:

$$\alpha_\mathrm{s} = \frac{\gamma_\mathrm{G}^2\tau_\mathrm{th}}{3\rho}\frac{CT\omega_\mathrm{s}^2}{v_\mathrm{s}^3}, \tag{6}$$

where C is the specific heat; ν_s is the sound velocity, ω_s is a frequency of the ultrasound wave, γ_G is the Grüneisen constant, and τ_th is the life time of a thermal phonon in the solid. An expression for the specific heat $C(T)$ can be easily derived from the free energy defined by equation (4).

Figure 6 shows the temperature dependence of the sound velocity calculated with our model. The parameters of the anharmonic potential were chosen in a way

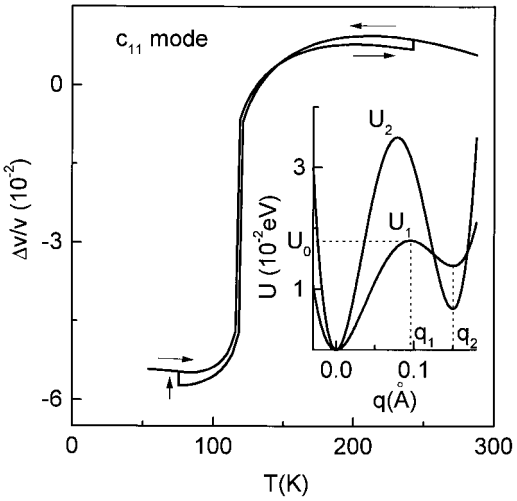

Fig. 6. Results of numerical calculation of the sound velocity versus temperature in $Ba_{1-x}K_xBiO_3$ (see text for details). Arrows show corresponding curves for temperature sweep up and down. Inset shows a double well potential for the oxygen octahedra used in simulations. The following parameters of the double-well potential were used $U_2(q)$: $U_0 = 0.035$ eV; $q_1 = 0.078$ Å; $q_2 = 0.15$ Å; $U_1(q)$: $U_0 = 0.018$ eV; $q_1 = 0.095$ Å; $q_2 = 0.15$ Å.

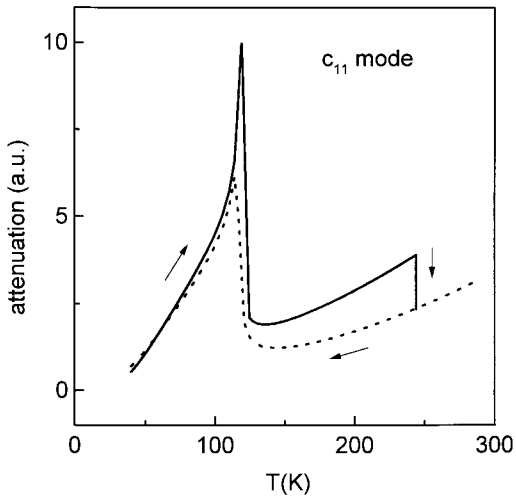

Fig. 7. Results of numerical calculation of the sound attenuation as a function of temperature (Eq. (6)) in $Ba_{1-x}K_xBiO_3$ (see text for details). Arrows have the same meaning as in Figure 6.

to describe correctly both softening of the sound velocity and the temperature region of the hysteresis. We would like to point out that our fitting values of the energy barrier $U_0 = 0.035$ eV and the distance between two positions of the minimum $q_2 = 0.15$ Å for the $U(q)$ agree well with the values determined from an analysis of the X-ray absorption spectra [11] $U_0 = 0.04$ eV and $q_2 = 0.16$ Å. It is important to note that in order to describe correctly the hysteretic behavior of the sound velocity we assume that some of the octahedra move in the modified double well potential $U_2(q)$. The double-well potential $U_2(q)$ is almost symmetrical whereas for $U_1(q)$ the one of the wells is weakly developed although the potential is strongly anharmonic (see insert of Fig. 6). But, as the numerical simulation revealed, the number of oxygen octahedra N_1 moving in the potential $U_1(q)$ far exceeds the number of octahedra N_2 moving in the potential $U_2(q)$ ($N_1/N_2 \approx 25$). The fact that some oxygen octahedra move in modified double well potential is not surprising. Evidently, there is some distribution of the double-well potential energy profile at the oxygen sites, depending on the local configuration of Bi(I)–Bi(II)–Bi(I) or Bi(I)–Bi(II)–Bi(II) atoms and on the local potassium occupation of the barium sites.

A relation between the coupling constants λ_3 and λ_4 determines the direction of path tracing of the hysteresis loop. In the case of the c_{11} mode $\lambda_3/\lambda_4 \approx 6.5$ and the cubic interaction prevails. An opposite tracing path takes place for the c_{44} mode below 120 K (see Fig. 4). In our model this fact is explained by another ratio between the coupling constants $\lambda_3/\lambda_4 \approx 3.5$. Calculated curves for the sound velocity and the attenuation of the c_{44} mode are quite similar (except for the direction tracing of the hysteresis loop) to the behavior of the c_{11} mode and they are not shown here.

Figure 7 shows a calculated temperature dependence (see Eq. (6)) of the sound attenuation. One can see rather good agreement with the experimental data (see Fig. 3). A peak in the attenuation stems from the motion of oxygen octahedra in the strongly anharmonic potential $U_1(q)$. Whereas a movement of some oxygen octahedra in $U_2(q)$ potential leads to the hysteresis in the sound velocity and the attenuation of sound. Numerical simulation shows that the hysteresis should not appear if one changes a temperature scan direction in the middle of the hysteretic area. One can clearly see this tendency in our experimental data (see lower curves in Fig. 2 and upper curves in Fig. 3). Apparently an increase of potassium concentration x changes the double-well potential parameters that leads to a decrease of the hysteresis loop width. We observed this in the $Ba_{0.53}K_{0.47}BiO_3$ compound (see Fig. 5).

It is interesting to compare $Ba_{1-x}K_xBiO_3$ to the A-15 superconducting compounds, where the electron-phonon interaction manifests itself through two alternative channels: the superconductivity and a structural phase transformation [23]. Many physical properties of $Ba_{1-x}K_xBiO_3$ are quite similar to physical properties of A-15 superconductors [23,35]. Examples are some structural instability, just above the superconducting state, a relatively high critical temperature (in comparison with conventional superconductors) of the superconducting phase transition, soft phonon modes (acoustic in A-15 compounds and optic in $Ba_{1-x}K_xBiO_3$), an anharmonicity of some phonons, and large softening of the elastic constants. It has been shown that an enhancement of T_c in A-15 compounds originates from a lattice instability which arose due to an anharmonicity of some phonon modes. An onset of the superconductivity in A-15 compounds arrests abruptly the growing structural instability and probably prevents the need for a structural transformation. If a structural

transition takes place it leads to a reduction in T_c [23,35]. The superconductivity survives below the structural phase transition in A-15 compounds, although it is not clear if a structural transformation happens in superconducting $Ba_{1-x}K_xBiO_3$. A-15 superconductors demonstrate neither hysteresis nor an abrupt change in temperature dependence of the sound velocity.

There are some models of a superconductor (see, for example, Refs. [36,37]) which consider explicitly the lattice anharmonicity and the lattice instability as a reason for the high critical temperature. Apparently, the mechanism suggested in these works cannot entirely be responsible for the superconductivity in $Ba_{1-x}K_xBiO_3$, since the estimates made in the frame of the BCS theory on the basis of harmonic phonons give reasonable values of T_c and the electron-phonon coupling constant λ_{ep}. However, in case of $Ba_{1-x}K_xBiO_3$ the anharmonic mechanism can give an additional contribution to forming the SC state and the electron-phonon coupling constant λ_{ep} can be enhanced due to the anharmonicity of some phonons associated with oscillations of oxygen octahedra.

4 Conclusions

We have carried out ultrasonic and low temperature X-ray powder diffraction experiments in the copper-free high temperature superconductors $Ba_{1-x}K_xBiO_3$ for two potassium concentrations $x \cong 0.35$ and $x \cong 0.47$. Large softening of the longitudinal and transverse elastic moduli confirms the existence of a lattice instability at temperatures slightly above the superconducting phase, although X-ray diffraction shows an absence of a structural phase transition down to 20 K within the resolution of our X-ray technique. Our theoretical model proceeding from the interaction of acoustic modes with movements of oxygen octahedra in a double well potential gives a good agreement with the experimental observations. We would like to point out that the existence of the anharmonic double-well potential can also be a reason for a local static distortion of the cubic structure. This case is encompassed by our theoretical consideration. Finally, a correlation between the local distortions can result in the structural phase transition.

In the context of all the statements made above we would like to emphasize that it is important to take the (local) structural instability into account in order to describe correctly the physical properties of $Ba_{1-x}K_xBiO_3$, including the origin of the SC state. Evidently the anharmonic phonons play a significant role in these compounds.

This acoustic investigation of the $Ba_{1-x}K_xBiO_3$ superconductor is a further example of the possible interplay of lattice properties and the superconductivity. Other examples investigated by our group are the cubic superconductor $CeRu_2$ [38], the Chevrel phase materials [39] and the stannides $Yb_3Rh_4Sn_{13}$ [40]. In all these cases softening of acoustic modes in the normal state is also important.

This work was supported in part by SFB 252. The work in Minsk was partly supported by INTAS organization under grant No. 97-1371. One of the authors (S.Z.) would like to thank the Alexander von Humboldt foundation for the financial support and members of the Physikalisches Institut der J.W. Goethe Universität for hospitality.

References

1. S. Pei, J.D. Jorgensen, B. Dabrowski, D.G. Hinks, D.R. Richards, A.W. Mitchell, J.M. Newsam, S.K. Sinha, D. Vaknin, J. Jacobson, Phys. Rev. B **41**, 4126 (1990).
2. D.G. Hinks, D.G. Richards, B. Dabrowski, D.T. Marx, A.W. Mitchell, Nature **335**, 419 (1988); S. Kondoh, M. Sera, Y. Ando, M. Sato, Physica C **157**, 469 (1989).
3. C.K. Loong, P. Vashishta, R.K. Kalia, M. H. Degani, D.L. Price, J.D. Jorgensen, D.G. Hinks, B. Dabrowski, A.W. Mitchell, D.R. Richards, Y. Zheng, Phys. Rev. Lett. **62**, 2628 (1989).
4. C.K. Loong, D.G. Hinks, P. Vashishta, W. Jin, R.K. Kalia, M.H. Degani, D.L. Price, J.D. Jorgensen, B. Dabrowski, A.W. Mitchell, D.R. Richards, Y. Zheng, Phys. Rev. Lett. **66**, 3217 (1991).
5. Q. Huang, J.F. Zasadzinski, N. Tralshawala, K.E. Gray, D.G. Hinks, J.L. Peng, R.L. Greene, Nature **347**, 369 (1990).
6. J.F. Zasadzinski, N. Tralshawala, D.G. Hinks, B. Dabrowski, A.W. Mitchell, D.R. Richards, Physica C **158**, 519 (1989).
7. J.F. Zasadzinski, N. Tralshawala, J. Timpf, D.G. Hinks, B. Dabrowski, A.W. Mitchell, D.R. Richards, Physica C **162-164**, 1053 (1989).
8. B. Batlogg, R.J. Cava, L.W. Rupp, Jr., A.M. Mujsce, J.J. Krajewski, J.P. Remeika, W.F. Peck, Jr., A.S. Cooper, G.P. Espinosa, Phys. Rev. Lett. **61**, 1670 (1988).
9. A. Puchkov, T. Timusk, M.A. Karlow, S.L. Cooper, P.D. Han, D.A. Payne, Phys. Rev. B **52**, R9855 (1995); A. Puchkov, T. Timusk, M.A. Karlow, S.L. Cooper, P.D. Han, D.A. Payne, Phys. Rev. B **54**, 6686 (1996).
10. L.F. Mattheiss, D.R. Hamann, Phys. Rev. Lett. **60**, 2681 (1988); N. Hamada, S. Massidda, A. J. Freeman, J. Redinger, Phys. Rev. B **40**, 4442 (1989); D.A. Papaconstantopoulos, A. Pasturel, J.P. Julien, F. Cyrot-Lackmann, Phys. Rev. B **40**, 8844 (1989).
11. A.P. Menushenkov, K.V. Klement'ev, P.V. Konarev, A.A. Meshkov, JETP Lett. **67**, 1034 (1998).
12. M. Shirai, N. Suzuki, K. Motizuki, J. Phys. Cond. Matter **2**, 3553 (1990); A.I. Liechtenstein, I.I. Mazin, C.O. Rodriguez, O. Jepsen, O.K. Andersen, M. Methfessel, Phys. Rev. B **44**, 5388 (1991); W. Jin, M.D. Degani, R.K. Kalia, P. Vashishta, Phys. Rev. B **45**, 5535 (1992).
13. K. Kunc, R. Zeyher, Phys. Rev. B **49**, 12216 (1994).
14. M. Braden, W. Reichardt, A.S. Ivanov, A.Yu. Rumyantsev, Europhys. Lett. **34**, 531 (1996); S.N. Barilo (private communication).
15. Y. Koyama, S.-I. Nakamura, Y. Inoue, Phys. Rev. B **46**, 9186 (1992).
16. H.D. Rosenfeld, T. Egami, in *Lattice Effects in High-T_c Superconductors*, edited by Y. Bar-Yam, T. Egami (World Scientific, Singapore, 1992), p. 105.

17. K.N. Mikhalev, S.V. Verkhovskii, A.P. Gerashchenko, Yu.V. Piskunov, A.Yu. Yakubovskii, A.P. Rusakov, JETP Lett. **70**, 346 (1999).
18. Y. Yacoby, S.M. Heald, E.A. Stern, Solid State Commun. **101**, 801 (1997).
19. M.-F. Xu, Y.J. Qian, K.J. Sun, Y. Zheng, Q. Ran, D. Hinks, B.K. Sarma, M. Levy, Physica B **165&166**, 1281 (1990); M. Levy, M.-F. Xu, B.K. Sarma, K.J. Sun, in *Physical Acoustics, Vol. XX*, edited by M. Levy (Academic Press, New York, 1992), p. 237.
20. S.N. Barilo, D.I. Zhigunov, L.A. Kurochkin, A.V. Pushkarev, S.V. Shiryaev, Sov. Phys. Supercond. **5**, 1081 (1992).
21. J. Marcus, C. Escribe-Filippini, S.K. Agarwal, C. Chaillout, J. Durr, T. Fournier, J.L. Tholence, Solid State Commun. **78**, 967 (1991).
22. B. Lüthi, G. Bruls, P. Thalmeier, B. Wolf, D. Finsterbusch, I. Kouroudis, J. Low Temp. Phys. **95**, 257 (1994).
23. L.R. Testardi, in *Physical Acoustics, Vol. X*, edited by W.P. Mason, R.N. Thurston (Academic Press, New York, 1974).
24. P. Kumar, D. Hall, R.G. Goodrich, Phys. Rev. Lett. **82**, 4532 (1999).
25. B.F. Woodfield, D.A. Wright, R.A. Fisher, N.E. Phillips, H.Y. Tang, Phys. Rev. Lett. **83**, 4622 (1999);
26. M. Levy, in *Physical Acoustics, Vol. XX*, edited by M. Levy (Academic Press, New York, 1992), p. 1.
27. T. Fukami, N. Inoue, S. Mase, J. Phys. Soc. Jpn **53**, 4322 (1984).
28. J.C. Slonczewski, H. Thomas, Phys. Rev. B **1**, 3599 (1970).
29. W. Henkel, J. Pelzl, K.-H. Höck, H. Thomas, Z. Phys. B **37**, 321 (1980).
30. P. Thalmeier, B. Lüthi, in *Handbook on the Physics and Chemistry of Rare Earths* (Elsevier Science Publishers B.V., 1991), Vol. 14.
31. D.N. Zubarev, *Nonequilibrium Statistical Thermodynamics* (Nauka, Moscow, 1971).
32. A.P. Saiko, V.E. Gusakov, V.S. Kuz'min, Low Temp. Phys. **20**, 764 (1994).
33. R.P. Feynman, *Statistical mechanics*, edited by J. Shaham (Benjamin Inc., Reading, Massachusetts, 1972).
34. R. Truell, C. Elbaum, B. Chick, *Ultrasonic Methods in Solid State Physics* (Academic Press, New York and London, 1969).
35. L.R. Testardi, Rev. Mod. Phys. **47**, 637 (1975).
36. G.M. Vujicic, V.L. Aksenov, N.M. Plakida, S. Stamenkovic, J. Phys. C **14**, 2377 (1981); N.M. Plakida, V.L. Aksenov, S.L. Drechsler, Europhys. Lett. **4**, 1309 (1987).
37. J.R. Hardy, J.W. Flocken, Phys. Rev. Lett. **60**, 2191 (1988).
38. B. Wolf, C. Hinkel, S. Holtmeier, D. Wichert, I. Kouroudis, G. Bruls, B. Lüthi, M. Hedo, Y. Inada, E. Yamamoto, Y. Haga, Y. Onuki, J. Low Temp. Phys. **107**, 421 (1997).
39. B. Wolf, J. Molter, G. Bruls, B. Lüthi, L. Jansen, Phys. Rev. B **54**, 348 (1996).
40. A. Haas, D. Wichert, G. Bruls, B. Lüthi, G. Balakrishnan, D. McK. Paul, J. Low Temp. Phys. **114**, 285 (1999).